JOURNAL OF MATERIALS SCIENCE **38** (2003) 1499–1505

Investigation of the interactions between two contact fibers in the fiber suspensions

JIANZHONG LIN*, ZHICHAO ZHANG
Department of Mechanics, State Key Laboratory of Fluid Power Transmission and Control, Zhejiang University, Hangzhou, 310027, People's Republic of China
E-mail: mecjzlin@yahoo.com

ZHAOSHENG YU
Department of Mechanical and Mechatronic Engineering, University of Sydney, NSW 2006, Australia

A mathematical model was constructed for the mechanical interactions between two contact fibers, based on which numerical simulations were performed and the results are in good accordance with the experiments. The settling fiber begins to slide at earlier time and the entire interaction duration diminishes as the initial position of the contact point, the initial orientation of fiber and the fiber specific weight increase or the solvent viscosity decreases. Both the slipping start-up time and the departing time delay as the fiber aspect ratio increases, however, the effect caused by reducing the diameter is more significant than that caused by increasing the length. Finally, a synthetic parameter which can uniquely describe the start-up time and the finishing time of the sliding motion of the fibers was derived.

Nomenclature

a_n	Axial acceleration of the contact point
a_t	Transverse acceleration of the contact point
a_ε	Relative acceleration of the center to the contact point, equals to $\dot{\omega}s$
A	Synthetic parameter
$\vec{F}(s)$	Line density of the Stokes force acting on the fluid by a fiber
$\vec{F}_c$	Contact force
F_{drag}	Drag acting on the fiber, equals to ηv
F_n	Normal component of contact force
F_t	Tangential component of contact force
F_x	Tangential component of the Stokes force
F_y	Normal component of the Stokes force
G	Difference of gravitation and buoyancy
I	Moment of inertia about the fiber center
l	Half length of fiber
L	Length of fiber
L_0	Characteristic length of fiber
m	Torque acting on the fiber
M	Mass of fiber
$\vec{n}$	A unit vector normal to both fibers
$\vec{p}$	Orientation of fiber, a unit vector
P_y	Component of $\vec{p}$, equals to $\cos\theta$
R	Radius of fiber
R_o	Radius at the fiber center
R_s	Radius of fiber at position s
R_0	Characteristic radius of fiber
S	Position along the fiber
S_c	Position of contact point
S_0	Position of initial contact point
υ	Velocity at contact point
$\vec{\upsilon}_o$	Translational velocity of the fiber
$\vec{\upsilon}_{\text{induce}}$	Induced velocity by fixed fiber
$\overrightarrow{\upsilon^\infty}$	Undisturbed velocity at $\vec{x}$
$\vec{x}$	Vector of position
$\vec{x}_0$	Position of fiber center
$\vec{\delta}$	Kronecker operator
ε	A quantity equals to $[\log(2l/R_0)]^{-1}$
η	Coefficient of drag
θ	Angle between fiber axis and horizontal
θ_0	Initial angle between fiber axis and horizontal
μ	Solvent dynamic viscosity
ν	Solvent kinematic viscosity
ν_0	Characteristic solvent viscosity
ρ	Specific weight of fiber
ρ_0	Characteristic specific weight of fiber
φ	Aspect ratio of fiber
ω	Angular velocity of fiber
$\dot{\omega}$	Angular acceleration of fiber
$\overrightarrow{\Omega}$	Vector of angular velocity of fiber

Subscript

c	Contact point
1	Fiber 1
2	Fiber 2

*Author to whom all correspondence should be addressed.

1. Introduction

The behavior of fibers in a flow affects the processing of composite materials or paper making. When the fiber concentration is higher, interactions between fibers have a profound effect on the microstructure of a suspension, and hence on its macroscopic properties. The presence of mechanical contacts between the fibers increases significantly the effective stress of the suspension. Numerical simulations indicated that the effective viscosity is enhanced due to mechanical contacts between the fibers [1]. Mechanical contacts between fibers could also give rise to many nonlinear rheological characteristics such as finite normal stress differences [2], yield stress [3], rod climbing [4] and shear thinning.

There have been some experimental research on the interactions between fibers. Andersson and Rasmuson [5] measured the friction of pulp and synthetic fibers in both air and water, and observed that the sliding fiber alternately sticks and slides as it was pulled upward, a behavior known as "stick-slide." Modifications of the classical, single-parameter law relating frictional resistance to normal force were found to improve agreement with experimental results. Stick-slip behavior and deviations from classical friction laws were also found by Lee [6] in measurements of interfacial shear strength of 25–35 μ diameter silica fibers. Zeng *et al.* [7] determined the friction coefficient governing contact between a sedimenting sphere and a neutrally buoyant sphere. Petrich and Koch [8] investigated the nature of the forces involved in mechanical contact between fibers in a fluid and the interaction between a polymeric fiber settling under the influence of gravity and a fixed strand of the same material, and the static coefficient of friction was found to be 0.38 ± 0.06 which is in good agreement with published data. Chaouche and Koch [9] examined the influence of adhesive contacts between fibers on rheology of suspension.

The interactions between fibers play an important role for the properties of fiber suspensions, in which the process and duration of interactions are crucial. Therefore, it is necessary to investigate the factors affecting the process and duration of interactions, these factors include the initial contact point, the aspect ratio and specific weight of fiber, the solvent viscosity. It is especially meaningful to generalize a synthetic parameter to describe the total interaction duration of the fibers. To the author's knowledge these important feature of fiber interactions have not been yet reported. The aim of this study is to construct a mathematical model for the mechanical interaction between two contact fibers, shed light on the effects of the fiber initial conditions, the fiber aspect ratio, specific weight and the solvent viscosity on the interactions between the fibers, and derive a synthetic parameter to describe the interaction duration of the fibers by performing numerical simulations.

2. Mathematical model

An illustration of the contact problem for two fibers is given in Fig. 1. One fiber is horizontally fixed and another fall from a very short distance above the fixed one. The track of the settling fiber can be represented by the profiles of P_y and S_c. The settling fiber's orientation is denoted by the unit vector $\vec{p}$. After contact, the settling fiber pivoted about the initial contact point. The fiber rotated in this manner until the tangential component of the gravitational force overcame static friction, so that the fiber began to slide along the horizontal fiber while rotating.

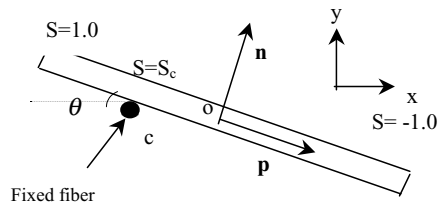

Figure 1 Side view of fiber interaction, with fixed fiber oriented perpendicular to the page.

We are interested in the problem at small Reynolds numbers for the settling fiber (less than 1×10^{-3}). Therefore, inertial can be neglected and the forces imposed on the settling fiber are assumed to be gravity, hydrodynamic Stokes drag [10] (including the long-range disturbance caused by the fixed fiber), and a contact force $\vec{F}_c$, which prevents the fibers from penetrating each other and provides a frictional resistance to the sliding motion.

According to Batchelor's slender-body theory [10], the velocity at the surface of the fiber is the superposition of the fluid's undisturbed velocity and the disturbed velocity due to the presence of the fiber which is in association with the Stokes force. Thus, for an isolated fiber, we have [11]:

$$\begin{aligned}
&\vec{v}_o + [\vec{\Omega} \times s\vec{p}] \\
&= \vec{v}_{\text{induce}}(\vec{x}_o + s\vec{p}) + \vec{v}^{\infty}(\vec{x}_o + s\vec{p}) \\
&= \frac{1}{4\pi\mu}\left(\frac{1}{\varepsilon} + \ln\frac{(1-s^2)^{\frac{1}{2}}}{R_s/R_0}\right)(\vec{\delta} + \vec{p}\vec{p})\cdot\vec{F}(s) \\
&\quad + (\vec{\delta} - 3\vec{p}\vec{p})\cdot\vec{F}(s) + (\vec{\delta} + \vec{p}\vec{p})\cdot\int_{-1}^{1}\frac{\vec{F}(s') - \vec{F}(s)}{|s-s'|}\mathrm{d}s' \\
&\quad + \vec{v}^{\infty}(\vec{x}_o + s\vec{p}) \qquad (1)
\end{aligned}$$

The line density of the Stokes force acting on the fluid by the fiber, $\vec{F}(s)$, can be then solved from Equation 1.

However, the presence of the horizontally fixed fiber will give rise to an additional disturbed velocity, hence we need to combine the integral equations of the two fibers. Denoting the settling fiber as 1 and the fixed fiber as 2, we write the combined equations as follows:

$$\begin{aligned}
&\vec{v}_{o1} + [\vec{\Omega}_1 \times s_1\vec{p}_1] \\
&= \frac{1}{4\pi\mu}\left(\frac{1}{\varepsilon} + \ln\frac{(1-s_1^2)^{\frac{1}{2}}}{R_s/R_0}\right)(\vec{\delta} + \vec{p}_1\vec{p}_1)\cdot\vec{F}_1(s_1) \\
&\quad + \frac{1}{8\pi\mu}(\vec{\delta} - 3\vec{p}_1\vec{p}_1)\cdot\vec{F}_1(s_1)
\end{aligned}$$

$$
\begin{aligned}
&+(\vec{\delta}+\vec{p}_1\vec{p}_1)\cdot\int_{-1}^{1}\frac{\bar{F}_1(s_1')-\vec{F}_1(s_1)}{|s_1-s_1'|}\mathrm{d}s_1'\\
&+\int_{-1}^{1}H(\vec{x}_{o2}+s_2\vec{p}_2-\vec{x}_{o1}-s_1\vec{p}_1)\cdot\vec{F}_2(s_2)\mathrm{d}s_2\\
&+\vec{\upsilon}^{\infty}(\vec{x}_{o1}+s_1\vec{p}_1)\vec{\upsilon}_{o2}+[\vec{\Omega}_2\times s_2\vec{p}_2]\\
=&\frac{1}{4\pi\mu}\left(\frac{1}{\varepsilon}+\ln\frac{\left(1-s_2^2\right)^{\frac{1}{2}}}{R_s/R_0}\right)(\vec{\delta}+\vec{p}_2\vec{p}_2)\cdot\vec{F}_2(s_2)\\
&+\frac{1}{8\pi\mu}(\vec{\delta}-3\vec{p}_2\vec{p}_2)\cdot\vec{F}_2(s_2)\\
&+(\vec{\delta}+\vec{p}_2\vec{p}_2)\cdot\int_{-1}^{1}\frac{\bar{F}_2(s_2')-\vec{F}_2(s_2)}{|s_2-s_2'|}\mathrm{d}s'\\
&+\int_{-1}^{1}H(\vec{x}_{o1}+s_1\vec{p}_1-\vec{x}_{o2}-s_2\vec{p}_2)\cdot\vec{F}_1(s_1)\mathrm{d}s_1\\
&+\vec{\upsilon}^{\infty}(\vec{x}_{o2}+s_2\vec{p}_2) \qquad (2)
\end{aligned}
$$

where H is a tensor function:

$$H(\vec{x})=\frac{1}{8\pi\mu}\left(\frac{\vec{\delta}}{|\vec{x}|}+\frac{\vec{x}\vec{x}}{|\vec{x}|^3}\right)$$

After discretization of the combined integral Equations 2 using Gauss-Legendre integral formulation, we obtain a set of linear algebra equations for the densities of the Stokes force on all Gauss points. By integrating these discrete forces, the resultant Stokes force as well as a torque about the center can be obtained. We decompose the resultant force into a tangential component F_x and a normal component F_y.

The settling fiber experiences two different stages. Firstly, it only pivots about the fixed fiber and secondly, it slides along the fixed fiber while rotating about it.

Fig. 2 shows the motion of the settling fiber and all forces on it in the first stage. F_x, F_y and m can be obtained through Gauss numerical integration method demonstrated above.

The dynamic equations of the settling fiber are:

$$\left.\begin{aligned}
&G\sin\theta+F_x-F_t=-M\omega^2 s\\
&G\cos\theta-F_y-F_n=M\dot{\omega}\cdot s\\
&m+F_n s=I\dot{\omega}
\end{aligned}\right\} \qquad (3)$$

where $I=MR^2/4+ML^2/3$. From Equation 3, $\dot{\omega}$, F_n, F_t can be determined and then we can judge whether the fiber will begin to slide from the values of F_n and F_t.

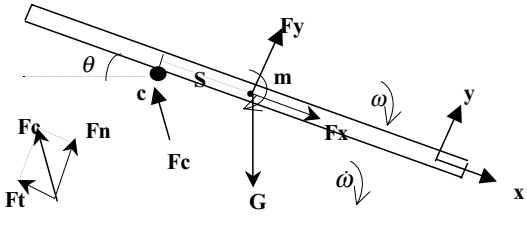

Figure 2 The motion of fiber and forces acting on the fiber in the first stage.

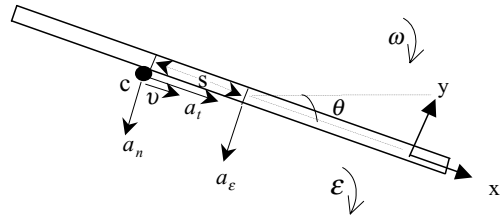

Figure 3 The motion of the fiber in the second stage.

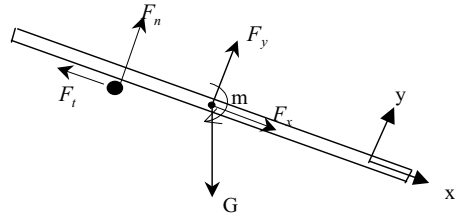

Figure 4 The forces on the fiber in the second stage

The fiber motion condition in the second stage is illustrated in Fig. 3. Fig. 4 shows all forces on the fiber. The fiber dynamic equations are as follows:

$$\left.\begin{aligned}
&G\sin\theta-F_x-F_t=M(a_t-\omega^2 s)\\
&G\cos\theta-F_y-F_n=M(a_n+\dot{\omega}\cdot s)\\
&m+F_n s=I\varepsilon\dot{\omega}
\end{aligned}\right\} \qquad (4)$$

There are five variables but only three equations in (4). Taking into account the frictional equation $F_t=\mu F_n+F_0$ we need one more equation. By analyzing the variation of velocity of the contact point c during a very small time step $\mathrm{d}t$, we obtain an approximate formulation for its transverse acceleration $a_n=\upsilon\omega$. Thus we can determine $\dot{\omega}$ and a_t from these five equations.

However, we should consider something more in our model. First, the slender-body theory regards the fiber that has a certain transverse dimension as a filament of zero thickness. Hence, the force obtained from Equation 2 has unavoidable errors. This finite transverse dimension of the fiber will result in a drag that is proportional to the fiber's longitudinal velocity. Second, when the two fibers approach very closely, there exist lubrication interactions between them, which are also proportional to the relative velocity between two fibers. Therefore, it is reasonable to incorporate an additional drag term $F_{\mathrm{drag}}=\eta v$ into our model.

From above analyses, once the initial contact position and angular velocity of the settling fiber are given, we can determine the fiber motion at any time, including its velocity and displacement In Fig. 5, the solid lines represent the numerical results and the symbols $\circ$ (P_y) and $\times$ (S_c) represent the experimental results. The fiber used in experiments is cellulose acetate propionate with the length of 3 mm and the diameter of 80 μm and the density of 1.222×10^3 kg/m^3. The fluid is silicon oil with the viscosity of 20 cSt and the density of 0.95×10^3 kg/m^3. In this study, we set η to be 1.24×10^{-4}.

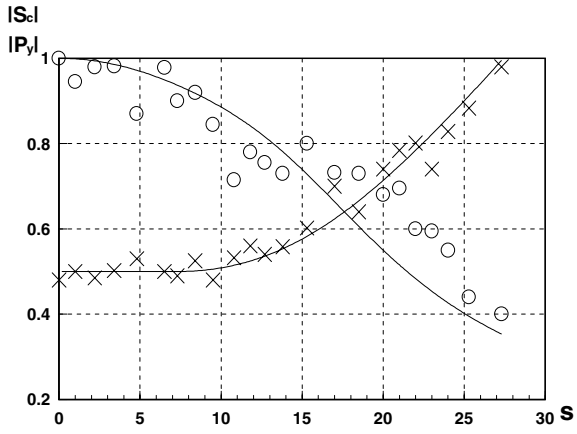

Figure 5 Comparison of the calculated results with the experiment ones.

3. Results and discussion

3.1. Effect of fiber initial conditions on the process of interaction

Fig. 6 shows the results for different initial contact positions S_0, and Fig. 7 for different fiber initial angle between axis and horizontal θ_0.

From Fig. 6 and Fig. 7, we can see that the settling fiber begins to slide at earlier time and the entire interaction duration diminishes as θ_0 or S_0 increases.

The orientation angles of the settling fiber at the time when it departs from the fixed fiber (referred to as departing angle) under different initial conditions are listed in Table I, which shows that the departing angle decreases as S_0 increases, but it largely remains the same when θ_0 varies in the range $0–30^0$.

We find that the results are basically independent of the initial angular velocity of the settling fiber. Thus

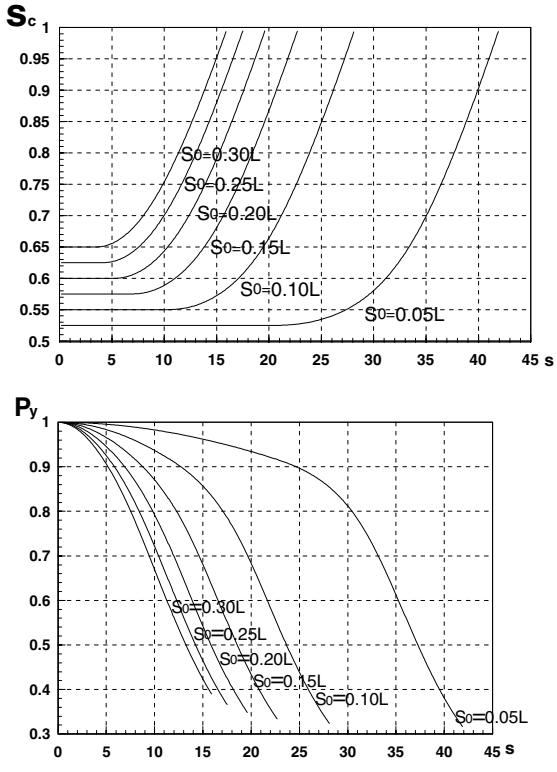

Figure 6 The results for the different positions of initial contact point of fibers.

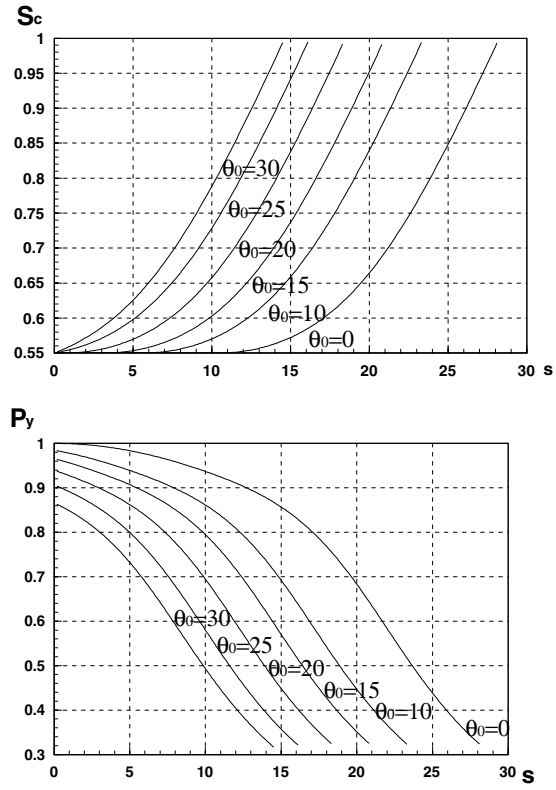

Figure 7 The results for the different fiber initial angle between axis and horizontal.

TABLE I The case under different initial conditions

S_0	$0.05l$	$0.10l$	$0.15l$	$0.20l$	$0.25l$	$0.30l$
Departing angle (°)	71.75	71.37	70.73	69.84	68.72	67.36
ϑ_0	0	10	15	20	25	30
Departing angle (°)	71.37	71.37	71.37	71.37	71.44	71.75

we can conclude that it is not the initial velocity but the initial position that has an appreciable effect on the subsequent interaction process.

3.2. Effect of fiber aspect ratio on the process of interaction

Different aspect ratios of the fiber $\varphi = L/R$ can be obtained by either changing the diameter of the fiber or the length. The results obtained by changing the length at the fixed radius of fiber $R = 40$ μm are depicted in Fig. 8 and those obtained by varying the diameter at the fixed length $2l = 3$ mm are shown in Fig. 9.

The starting times of the slipping motion, the finishing times (departing time) and the departing angles for both cases are listed in Table II, in which φ_l and φ_r represent aspect ratio when changing the fiber length and diameter respectively.

We can see that both the slipping start-up time and the departing time delay as the fiber aspect ratio increases, no matter whether it is caused by increasing the length or by decreasing the diameter. Nevertheless, the effect caused by varying the diameter is more significant and

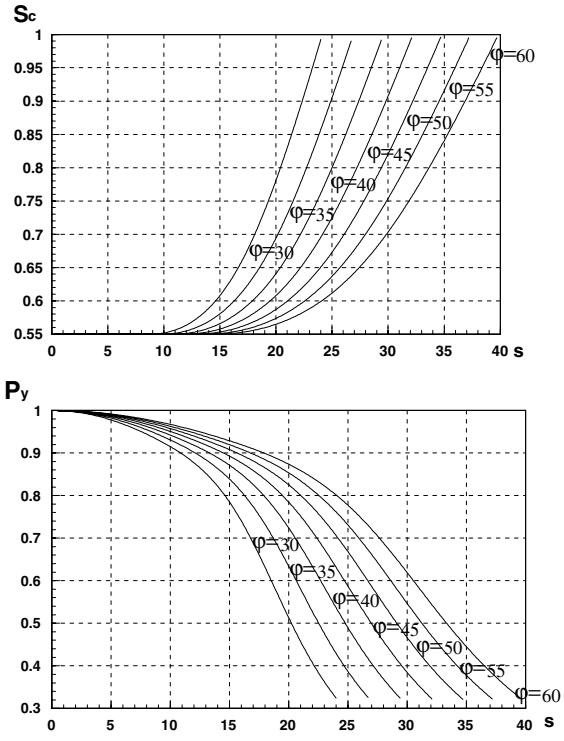

Figure 8 Results for different aspect ratios of the fiber by changing the fiber length only.

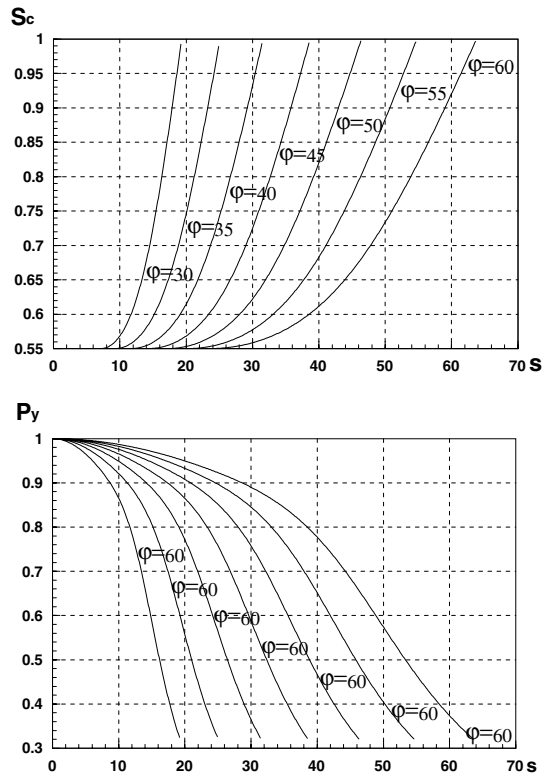

Figure 9 Results for different aspect ratios of the fiber by changing the fiber diameter only.

the delay rate seems higher at a higher aspect ratio, whereas it seems higher at a lower aspect ratio in case of varying the diameter. Therefore, the fiber aspect ratio φ is not an independent parameter for the interaction process.

3.3. Effect of solvent viscosity and fiber density on the interaction process

The results for different fiber specific weight and different solvent viscosities are shown in Figs 10 and 11 respectively.

The slipping start-up times, the departing times and the departing angles for both cases are listed in Table III.

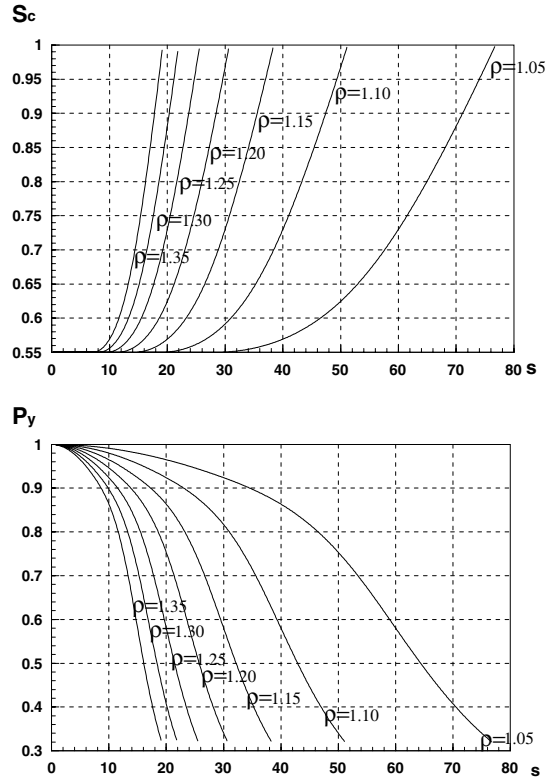

Figure 10 Results for different fiber specific weight (10^3 kg/m^3).

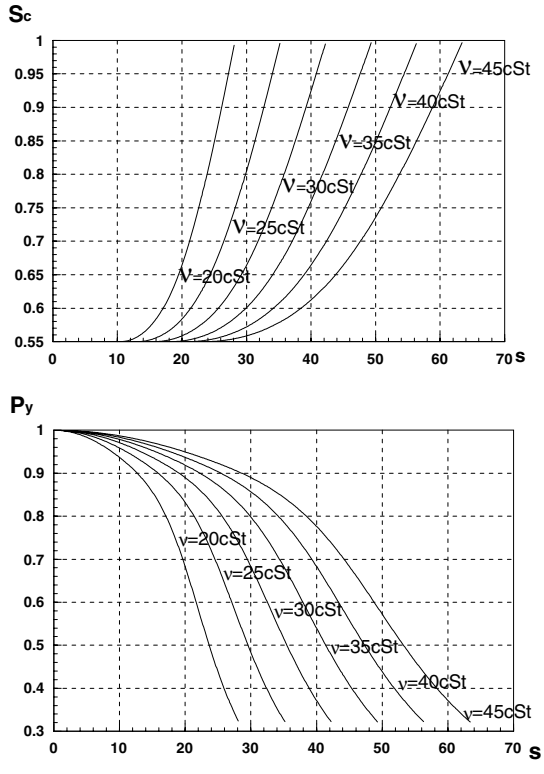

Figure 11 Results for different solvent viscosities (1cSt = 0.01, St = 0.01cm^2/s).

TABLE II The case for different aspect ratios of the fiber

φ_l	30	35	40	45	50	55	60
Start-up (slipping) time (s)	8.90	9.91	10.89	11.86	12.80	13.73	14.64
Departing time (s)	24.13	26.89	29.58	32.22	34.80	37.34	39.84
Departing angle (°)	71.34	71.36	71.37	71.39	71.40	71.41	71.42
φ_r	30	35	40	45	50	55	60
Slipping start-up time (s)	7.12	9.25	11.62	14.23	17.07	20.13	23.42
Departing time (s)	19.30	25.09	31.56	38.66	46.40	54.77	63.75
Departing angle (°)	71.34	71.36	71.37	71.39	71.40	71.41	71.42

TABLE III The case for different fiber specific weight and different solvent viscosities

ρ	1.05	1.10	1.15	1.20	1.25	1.30	1.35
Slipping start-up time (s)	28.30	18.87	14.15	11.32	9.43	8.09	7.07
Departing time (s)	76.82	51.22	38.41	30.73	25.61	21.95	19.21
Departing angle (°)	71.37	71.37	71.37	71.37	71.37	71.37	71.37
ν	20cSt	25cSt	30cSt	35cSt	40cSt	45cSt	
Start-up(slipping) time (s)	10.40	13.00	15.61	18.21	20.81	23.41	
Departing time (s)	28.24	35.31	42.37	49.43	56.49	63.55	
Departing angle (°)	71.37	71.37	71.37	71.37	71.37	71.37	

It shows that the settling fiber begins to slip earlier and departs from the fixed fiber earlier as the fiber specific weight increases or the solvent viscosity decreases, but the departing angle is not affected by the fiber specific weight and the solvent viscosity.

3.4. The synthetic parameter containing the properties of the fiber and the fluid

The length, radius, specific weight of the fiber and the solvent viscosity are involved in the interactions between the fibers. We attempt to derive a synthetic parameter A which contains these quantities, allowing the slipping start-up time to be expressed as $t_0 = f(A)$ and the total duration of interaction between the fibers as $T = g(A)$.

We non-dimensionlize the length L, the radius R, the fiber specific weight ρ and the solvent viscosity ν using the characteristic quantities: $L' = L/L_0$, $R' = R/R_0$, $\nu' = \nu/\nu_0$, $\rho' = \rho/\rho_0$. Data in Table IV are calculated using data in Table III.

From Table IV, we can see that the slipping start-up time and the departing time change linearly with ν'. Therefore, we assume

$$A = \frac{\nu' l'^{\alpha}}{R'^{\beta}\rho'^{\gamma}} \tag{5}$$

Similarly we can calculate the slipping start-up time and the departing time when the length L, the radius R or the specific weight $\rho$of the fiber change. The results are shown in Tables V–VII.

Based on the results of Tables V–VII, we can obtain the α, β and γ in the Equation 5, which then can be written as:

$$A = \frac{\nu' L'^{0.728}}{R'^{1.725}\rho'^{5.660}} \tag{6}$$

TABLE IV The results calculated using data in Table III

ν'	1.0000	1.2500	1.5000	1.7500	2.0000	2.2500
Slipping start-up time (s)	10.40	13.00	15.61	18.21	20.81	23.41
Departing time (s)	28.24	35.31	42.37	49.43	56.49	63.55
$\Delta\nu'$	1.00–1.25	1.25–1.50	1.50–1.75	1.75–2.00	2.00–2.25	
Delay of start-up time (s)	2.60	2.61	2.60	2.60	2.60	
Delay of the departing time (s)	7.06	7.06	7.06	7.06	7.06	

TABLE V The calculated results when half length L of the fiber changes

L'	0.8000	0.9333	1.0667	1.2000	1.3333	1.4667	1.6000
Slipping start-up time (s)	8.90	9.91	10.89	11.86	12.80	13.73	14.64
Departing time (s)	24.13	26.89	29.58	32.22	34.80	37.34	39.84

TABLE VI The calculated results when the radius R of the fiber changes

R'	1.2500	1.0714	0.9375	0.8333	0.7500	0.6818	0.6250
Slipping start-up time (s)	7.12	9.25	11.62	14.23	17.07	20.13	23.42
Departing time (s)	19.30	25.09	31.56	38.66	46.40	54.77	63.75

TABLE VII The calculated results when the specific weight ρ of the fiber changes

ρ'	0.8592	0.9002	0.9411	0.9820	1.0229	1.0638	1.1047
Slipping start-up time (s)	28.30	18.87	14.15	11.32	9.43	8.09	7.07
Departing time (s)	76.82	51.22	38.41	30.73	25.61	21.95	19.21

From Equation 6, we can see that the specific weight of the fiber has the largest effect on the interaction between the fibers.

4. Conclusions

Based on the results and discussions above, the following conclusions can be drawn:

(i) The initial position of the contact point S_0 and the initial orientation angle θ_0 have significant effects on the interaction process of two fibers. The settling fiber begins to slide at earlier time and the entire interaction duration diminishes as θ_0 or S_0 increases.

(ii) The fiber aspect ratio φ is not an independent parameter involving in the interaction between the fibers. Both the slipping start-up time and the departing time delay as the fiber aspect ratio increases, however, the effect caused by reducing the diameter is more significant than that caused by increasing the length.

(iii) The settling fiber begins to slip earlier and departs from the fixed fiber earlier as the specific weight of the fiber increases or the solvent viscosity decreases, but the departing angle is not affected by the fiber specific weight and the solvent viscosity.

(iv) A synthetic parameter A is derived to uniquely describe the slipping start-up time and the total interaction duration of the fibers.

Acknowledgements

The author are grateful to the National Natural Science Foundation for Outstanding Youth of China (No. 19925210) for financial support.

References

1. R. R. SUNDARAJAKUMAR and D. L. KOCH, *J. Non-Newtonian Fluid Mech.* **73** (1997) 205.
2. L. F. CARTER, PhD thesis, University of Michigan, Ann Arbor, MI, 1967.
3. C. P. J. BENNINGTON, R. J. KEREKES and J. R. GRACE, *Can. J. Chem. Eng.* **68** (1990) 748.
4. M. A. ZIRNSAK, D. U. HUR and D. V. BOGER, *J. Non-Newtonian Fluid Mech.* **54** (1994) 153.
5. S. R. ANDERSSON and A. RASMUSON, *J. Pulp Pap. Sci.* **23** (1997) J5.
6. I. LEE, *J. Mater. Sci.* **30** (1995) 6019.
7. S. ZEHG, E. T. KERNS and R. H. DAVIS, *Phys. Fluids.* **8** (1996) 1389.
8. M. P. PETRICH and D. L. KOCH, *ibid.* **10** (1998) 2111.
9. C. MOHEND and D. L. KOCH, *J. Rheology* **45** (2001) 369.
10. G. X. BATCHELOR, *J. Fluid Mech.* **44** (1970) 419.
11. M. B. MACKAPLOW and E. S. G. SHAQFEH, *ibid.* **329** (1996) 155.

Received 1 March
and accepted 13 December 2002